Network: Computation in Neural Systems
September 2007; 18(3): 213–233

informa
healthcare

Seasonal variations in the color statistics of natural images

MICHAEL A. WEBSTER, YOKO MIZOKAMI*,
& SHERNAAZ M. WEBSTER

*Department of Psychology, University of Nevada, Reno,
Reno NV 89557, USA*

(Received 22 March 2007; accepted 29 August 2007)

Abstract
We examined how the distribution of colors in natural images varies as the seasons change. Images of natural outdoor scenes were acquired at locations in the Western Ghats, India, during monsoon and winter seasons and in the Sierra Nevada, USA, from spring to fall. The images were recorded with an RGB digital camera calibrated to yield estimates of the *L*, *M*, and *S* cone excitations and chromatic and luminance contrasts at each pixel. These were compared across time and location and were analyzed separately for regions of earth and sky. Seasonal climate changes alter both the average color in scenes and how the colors are distributed around the average. Arid periods are marked by a mean shift toward the $+L$ pole of the *L* vs. *M* chromatic axis and a rotation in the color distributions away from the *S* vs. *LM* chromatic axis and toward an axis of bluish–yellowish variation, both primarily due to changes in vegetation. The form of the change was similar at the two locations suggesting that the color statistics of natural images undergo a characteristic pattern of temporal variation. We consider the implications of these changes for models of both visual sensitivity and color appearance.

Keywords: *Natural scenes, visual system*

Introduction

Many aspects of color vision have been attributed to adaptations to the natural color environment. For example, the spectral sensitivities of the receptors and of

Correspondence: Michael A. Webster, Department of Psychology, University of Nevada, Reno, Reno NV 89557, USA.
E-mail: mwebster@unr.nevada.edu
*Current address: Graduate School of Advanced Integration Science Chiba University 1-33 Yayoicho, Inage-ku, Chiba 263-8522, Japan

ISSN 0954-898X print/ISSN 1361-6536 online/07/030213–233 © 2007 Informa UK Ltd.
DOI: 10.1080/09548980701654405

post-receptoral channels may be optimized for efficiently representing color contrasts in natural scenes, and may also be optimized for specific visual tasks such as finding ripe fruit among foliage or judging the complexion and health of conspecifics (Polyak 1957; Mollon 1989; Osorio and Bossomaier 1992; Nagle and Osorio 1993; Osorio and Vorobyev 1996; Ruderman et al. 1998; Dominy and Lucas 2001; Regan et al. 2001; Changizi et al. 2006; Fernandez and Morris 2007). Salient features of color appearance may also reflect important characteristics of the environment, though somewhat paradoxically, they are not predicted from visual sensitivity, even though sensitivity itself is assumed to be matched to the environment. For example, the colors that appear as perceptual nulls (such as unique yellow which is the null for red vs. green sensations) do not represent the null points of the opponent channels mediating color coding at early post-receptoral levels of the visual system (Krauskopf et al. 1982), nor are they tied to individual differences in spectral sensitivity (Schefrin and Werner 1990; Miyahara et al. 1998; Brainard et al. 2000; Webster et al. 2000; Mizokami et al. 2006). This has suggested that the unique hues appear special because they represent special features of the environment. For example, unique blue and yellow lie very close to the axis along which natural daylights vary and may thus reflect a perceptual representation of the daylight locus (Lee 1990; Shepard 1992; Mollon 2006). Similarly, basic color terms, which are the primary landmarks of how colors are named by a language, have yet to find an account in terms of the known physiological processes in color coding, but have been predicted by analyzing the distribution of colors or lightness levels in images (Yendrikhovskij 2001; Attewell and Baddeley 2007), or the non-uniform structure of surface reflectances (Philipona and O'Regan 2006) or perceptual color space (Regier et al. 2007).

Given that the color characteristics of the environment may largely determine color coding, it is of obvious interest to characterize the colors in the environment. A number of studies have now measured the color statistics of natural images and have related these to visual coding (Burton and Moorhead 1987; Webster and Mollon 1997; Ruderman et al. 1998; Nascimento et al. 2002; Párraga et al. 2002; Johnson et al. 2005; Lovell et al. 2005; Long et al. 2006). Many of these have focused on the characteristic colors of scenes, by averaging the color distributions across individual images. In this study, our aim was to instead examine the variations in image color, by asking how color distributions change across scenes. These variations have important implications for understanding how consistent the environment may be in presenting specific color properties to the observer, and for understanding the time course or specific contexts in which color coding might have incorporated these properties. Variations in images are also important for understanding the nature of short-term visual adaptations to color, since they provide a measure of the stimulus range over which the visual system must operate, and thus a measure of how different color coding might be in different contexts.

In a previous study, we explored variations in the color of natural outdoor images and how observers are adapted to these by sampling the color statistics from scenes collected in different environments (Webster and Mollon 1997). In the present study, we focused on characterizing the variation in color within an environment, by asking how color distributions change as the seasons change. Seasonal changes in color are often perceptually dramatic because of changes in climate and vegetation. These variations are of interest because they represent

the range of colors a non-migrating species must face, and thus constrain how well a static visual system could represent colors from its environment. They also reveal the color cues that are available for judging the seasons or ''state'' of an environment.

Methods

Seasonal changes were measured at two locations, in the United States and India. These were chosen as part of a broader psychophysical project examining color appearance in different environmental contexts (Webster et al. 2002a, 2002b), and were collected over a period of several years from 2000 to 2005. The location in India was in a rural agricultural area within the Sayadhri mountain range of the Western Ghats in Nashik District, Maharashtra, a subtropical zone of montane rainforest and grasslands that undergoes an extreme cycle of rainfall with the annual monsoon. Images from this area included both close-range and panoramic views of valley and hills with both natural vegetation and cultivated rice fields and had few manmade objects. The images were acquired at two times: in September to early October near the end of the wet (monsoon) season, and from December to January during the dry (winter) season. The second set of images was acquired in the Toiyabe and Tahoe National Forests in the Sierra Nevada mountains near Reno, Nevada. These images included views of pine forests and meadows and again avoided obvious manmade structures. The Eastern Sierras are an area of relatively low annual precipitation (from <20 to <100 cm/year depending on elevation, compared to >400 cm/year in the Nashik location) but high altitude, and receive heavy snow accumulations at higher elevations during the winter. We sampled the scenes from May to October, between the periods of snow cover during which the measurement locations were not accessible. Examples of images from the two environments are shown in Figure 1. As far as possible we attempted to measure similar sets of views across the different times.

Images were acquired with an RGB digital camera (Sony DSC-D770), and thus provided colorimetric measurements of the scenes rather than the actual spectra. Spectral measurements based on multispectral imaging (Brelstaff et al. 1995; Webster and Mollon 1997; Ruderman et al. 1998; Nascimento et al. 2002) have the advantage that they provide more complete information about the underlying color signals and are less prone to errors in estimating the cone responses from the (different) spectral sensitivities of the camera sensors. However, colorimetric measurements can provide reasonable approximations of the cone excitations for naturalistic color signals and do not suffer from errors introduced by successively sampling the scenes at different wavelengths over time, and have now been used by a number of different groups for evaluating scene statistics and human color vision (Burton and Moorhead 1987; Párraga et al. 2002; Doi et al. 2003; Johnson et al. 2005; Lovell et al. 2005; Long et al. 2006).

For our measurements each image included a reference palette of known reflectance placed in the bottom right corner of the scene. For India we used the MacBeth Color Checker, while the later Sierra scenes were instead recorded using the MacBeth Color Checker DC, which includes a much more extensive palette of 206 distinct chips. Both palettes include a range of chips characteristic of natural

Figure 1. Examples of panoramic images from the Western Ghats and Sierras. The upper pair shows a valley near Trimbukeshwar during the monsoon (a) or winter (b) season. The lower pair shows images of Dog Valley in the spring (c) or fall (d).

colors with broad and smoothly varying spectra that are similar to the band-limited reflectance spectra for natural objects (Maloney 1986). During image capture the spectral power distribution reflected from the brightest white chip in the palette was also recorded with a PR650 spectroradiometer in order to measure the scene illuminant. This also allowed us to estimate the color signal for each chip in the palette (i.e. by multiplying the illuminant spectrum by each chip's reflectance spectrum).

The images were calibrated in the following steps. RGB values were first adjusted for the measured intensity response function of the sensors and then averaged over 2×2 pixel blocks (giving an image of 672 by 512 pixels). For each chip we calculated the *L*, *M*, and *S* cone excitation by weighting the chip color signal by the Smith and Pokorny cone sensitivities (Smith and Pokorny 1975), and obtained the corresponding RGB value by averaging over a block of pixels within the chip. The *LMS* cone excitations for each pixel in the image could then be estimated by interpolating the RGB values at each pixel between the known RGB values in bounding sets of color checker chips. For this the program identified sets of four reference chips that enclosed the pixel color with the smallest volume in RGB space. The accuracy of the calibration was assessed by predicting the set of chips in the Color Checker DC from the reference palette provided by the 24 chips in the

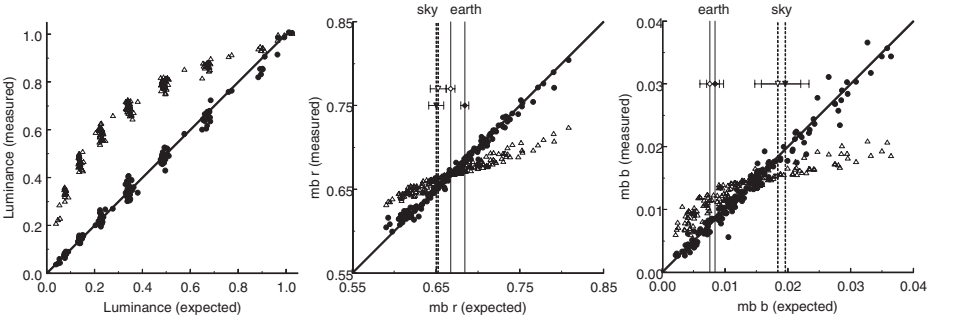

Figure 2. Predicted responses to the palette of matte chips in the Color Checker DC in an image calibrated based on the chips in the original Color Checker. Plots show the measured vs. expected values for the chip's luminance (left panel) and chromaticity in the MacLeod–Boynton (1979) color space (*L* vs. *M* or "*r*" coordinate, middle panel; *S* vs. *LM* or "*b*" coordinate, right panel). Filled circles and unfilled triangles plot the predictions in the calibrated and original uncalibrated images, respectively. Vertical lines with error bars show the average estimated chromaticity for earth (solid lines) and sky (dashed lines) regions in the images from India during the monsoon (unfilled diamonds) and winter (filled diamonds) seasons.

original Color Checker (in images that included both palettes). rmsError was roughly 2% of the maximum response in the *L* and *M* cone responses and was roughly 3% for the *S* cones. Figure 2 shows an example of the estimated luminance and chromaticity of chips in the Color Checker DC based on the image calibrated for the original Color Checker. Errors in chromaticity were generally larger for chips with high saturation (colors which were rare in the measured scenes) and for the darkest chips (i.e. low reflectance spectra at which chromaticity becomes poorly defined).

The calibrated color coordinates were stored as bitmap images in which the cone excitations at each point could be read out directly from the RGB values (with the values normalized for the maximum luminance for each scene). The results reported are based on an analysis of 664 images (113 in the Western Ghats and 551 in the Sierras). The data set is available on request from the authors.

Results

For each image, we examined the mean chromaticity in the scene and the principal axes (color-luminance directions) along which colors in the scene varied. These were used to compare differences in the color distributions across the seasons, the contribution of earth and sky to these changes, and the contribution of illumination vs. reflectance differences to the seasonal changes. Regions of earth or sky were demarcated manually by drawing boundaries into the calibrated images. The color statistics could then be estimated separately within these boundaries.

Figure 3 plots the aggregate probability distributions of color for the scenes measured in India and in the Sierras (in Dog Valley). The plots show the frequency of chromaticities within the MacLeod–Boynton (1979) color space. In this space, variations in the *b* axis represent signals in the *S* cones at constant luminance, and

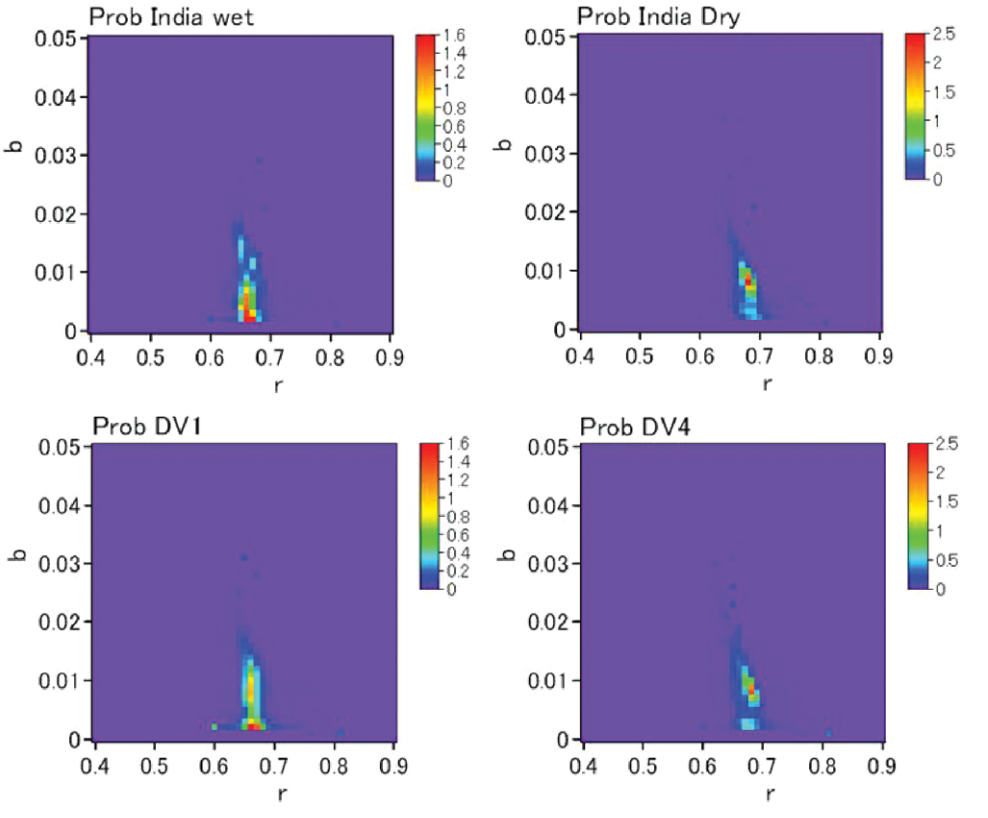

Figure 3. Probability density for color for scenes in India or the Sierras (Dog Valley) during wet or arid seasons. Plots show the distribution of chromaticities within the MacLeod–Boynton (1979) color space, and are based on averaging across individual scenes from a single location and time period.

are given by $S/(L+M)$, where S, L, and M are the cone responses at each individual pixel and the pixel's luminance is assumed to equal the sum of the L and M responses. Variations along the r axis represent the opposing signals in the L and M cones at constant luminance, and are given by $L/(L+M)$ at each pixel. These two axes have the advantage that they correspond to the two "cardinal axes" along which color is processed at retinal and geniculate stages of the primate visual system (Derrington et al. 1984). For reference, an equal energy white (illumant E) in the MacLeod–Boynton (1979) space has r and b coordinates of 0.6656 and 0.01545, respectively. The modal values for the distributions clearly peak at lower b values indicating that the scenes were on average more greenish or yellowish. The left and right panels in the figure show the distributions measured at the same location during either wet or dry seasons. Two differences are evident from these plots. First, the mean color shifts in the dry season toward higher r ($+L/-M$) values. Second, the distributions become more tilted in the color space. Specifically, during the wet season the colors tend to vary primarily along the b axis, while in the dry season there is a negative correlation in the signals along the two axes. In the following analyses we consider these color shifts in detail.

Figure 4 plots the average chromaticity for the scenes, this time showing the means for each individual scene within the sampled locations. The left panel summarizes measurements from India, while the right three panels show the results for three different locales in the Sierras. These are shown separately for clarity because the Sierra regions were sampled more frequently over time and because the three areas differed in elevation (from ~5500 ft for Dog Valley up to 8000 ft for Tahoe Meadows) and consequently had different temporal patterns for the color changes. For example, measurements at Tahoe Meadows do not show the monotonic shifts in average color that are seen in the Dog Valley and Boca locations, since the earliest measurements (in June) were still under some snow cover and thus a spring-like distribution did not emerge until the July measurements. In the upper panels of Figure 4 the mean chromaticity is shown separately for earth (large symbols) and sky (small symbols). In the lower panels the averages for earth are replotted but this time they are compared to the mean chromaticity for the illuminants (small symbols). Again, the scene illuminants were acquired from spectroradiometric measurements of the brightest white chip on the color checker. The chromaticities of the illuminants were more variable for the scenes in India because they included both clear and overcast days. However, for both locations the illuminant colors tend to lie within a ''gap'' separating the average color of sky and earth.

Several notable features are evident from these plots. First, for both environments the terrestrial regions of the images have a strong bias in average color, varying from greenish to yellowish depending on the season. Thus, in general, the earth is not gray (Brown 1994), and the achromatic point more closely corresponds to the average chromaticity for sky and earth. Second, there are pronounced changes in the average color with the seasons, and these show a different pattern for sky and earth. Regions of sky in the scenes tended to cluster tightly along a blue–yellow axis close to the blackbody locus. Compared to India, sky colors in the Nevada locations were more strongly shifted toward blue and also showed more obvious seasonal shifts presumably because of the higher northern latitude. For earth regions in both locations, the seasonal color change is largely manifested as a shift along the r axis or L vs. M chromatic dimension, with comparatively weak shifts along the S chromatic dimension. In the extreme this drives the mean earth color toward the blackbody locus so that it becomes continuous with the sky distribution. This shift, reflecting changes in the chlorophyll content of the vegetation, represents the dominant source of color changes in the images. That is, the long-term changes in environmental color at each location are primarily due to changes in the reflectances of the surfaces rather than to changes in the illuminants. Figure 4 also shows that the magnitude of the color change is greater for scenes with a lower mean b (S cone) signal, presumably because these scenes included a denser representation of vegetation. Finally, while the seasonal color shifts were more pronounced for the scenes measured in India, the pattern is qualitatively similar for the Sierras. That is, in both these disparate environments there is a characteristic shift in color along the L vs. M axis as the characteristic colors of the grasses and foliage changed.

Figure 5 directly compares the average chromaticity of the earth and sky regions of scenes from India to the incident illumination (at least as measured by the illumination incident on the reference chip). This again illustrates that changes in illumination were not the primary source of the color changes across the seasons,

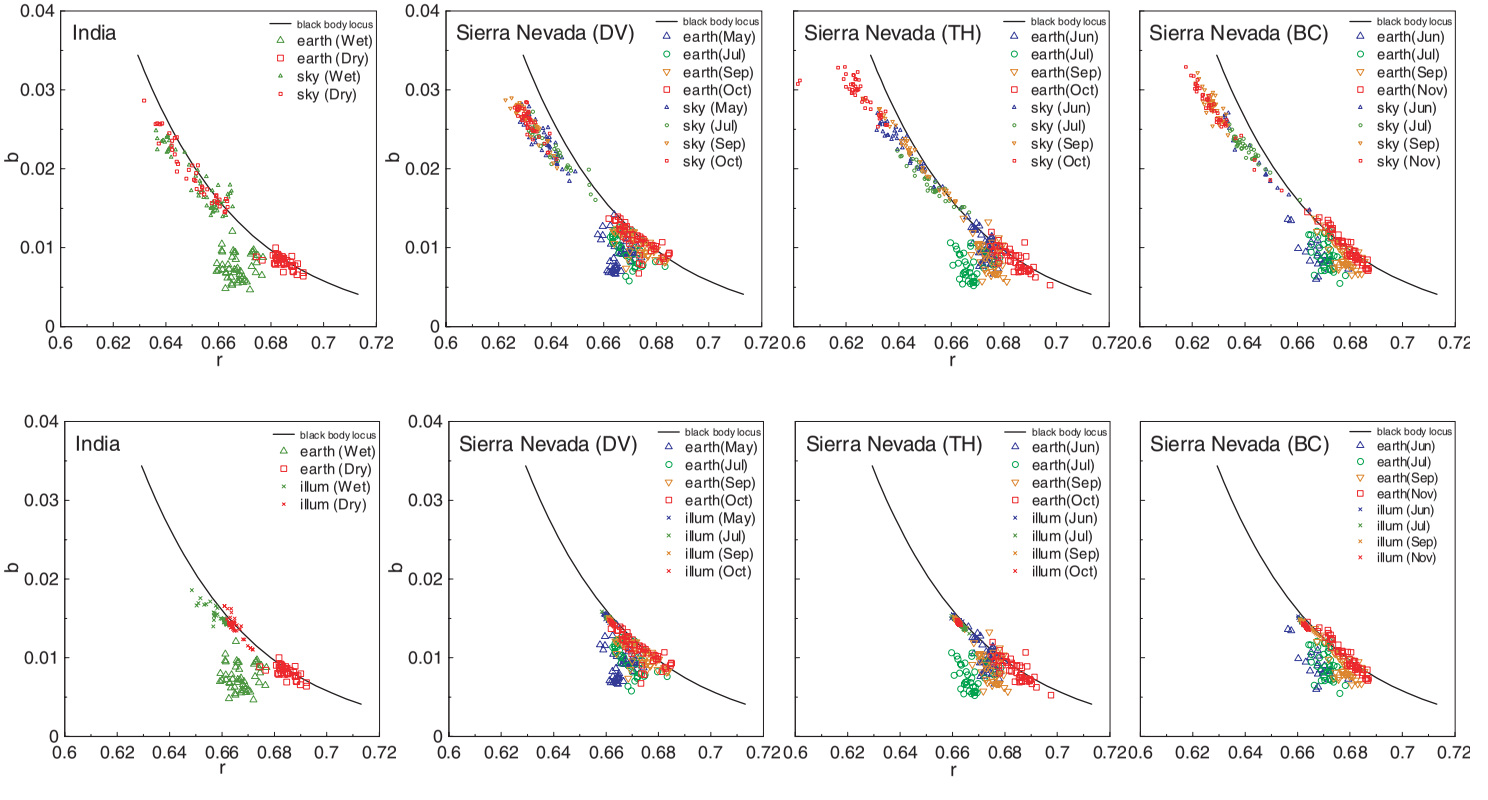

Figure 4. Mean chromaticities for earth, sky, and illuminants for individual scenes. Each panel shows the average chromaticities for scenes measured at a given location, with the measurement period shown by symbol color. The upper panels compare the mean color for regions of earth (large symbols) or sky (small symbols). The lower panels replot the means for earth regions (large symbols) along with the mean chromaticity of the illumination for each scene (small symbols).

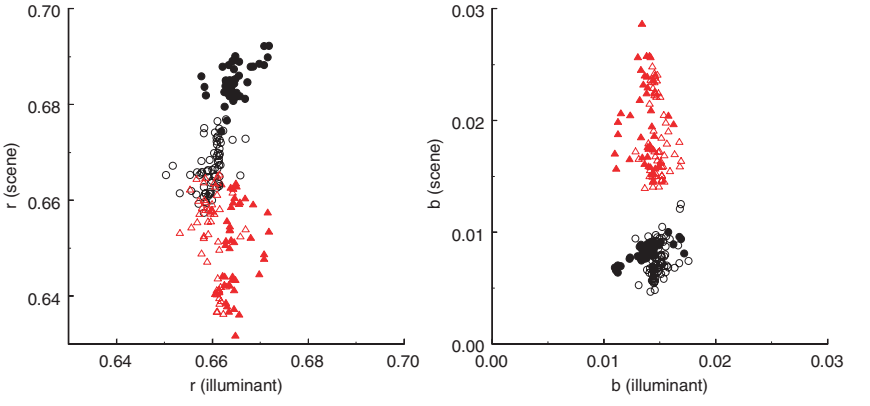

Figure 5. Mean chromaticity of scenes compared to the chromaticity of the illuminant, for the scenes measured in India. Left panel shows the MacLeod–Boynton (1979) *r* coordinate of the illuminant (*x* axis) and for the average of the regions of earth (black circles) or sky (red triangles). Filled and unfilled symbols are for winter and monsoon images, respectively. The right panel shows the corresponding comparisons for the *S* axis or *b* coordinate of the MacLeod–Boynton space.

and in particular, variations in the *L* vs. *M* component of the illuminant color were small relative to the *L* vs. *M* shift in the mean color of the terrain between the two seasons. Not surprisingly, though, the colors from scenes did depend on the illuminant within each time period. Correlations between the mean earth and illuminant *r* and *b* chromaticity were 0.61 (*r*) and 0.81 (*s*) for the images in winter and 0.49 (*r*) and 0.37 (*s*) in the monsoon set. However, this again suggests that a substantial source of the variation in average color across individual scenes is due to the sets of surfaces in the scenes. (On the other hand, it should be noted that images were acquired during midday and therefore did not reflect the full range of daily variation in illuminant chromaticity.)

As we noted above, the color distributions in Figure 3 show not only a change in average color but also in how the colors are distributed around the average within wet or dry periods. To examine this, we measured the principal axes of the color distributions for each scene, following an analysis similar to that described in Webster and Mollon (1997). However, in the present case we excluded regions of sky from the analysis, in order to focus on changes in the distribution of surface reflectances over time. The cone responses were first normalized for the average color and luminance of the scene, equivalent to von Kries scaling of the cone responses so that the average response to each scene equaled the response to a reference chromaticity of illuminant *C*. Next, contrasts relative to the mean along the three cardinal axes (*L* vs. *M*, *S* vs. *LM*, and the achromatic axis) were scaled to roughly equate signals along the three dimensions according to the following equations:

$$L \text{ vs. } M = 1955 \times (r - 0.6568)$$
$$S \text{ vs. } LM = 5533 \times (b - 0.01825)$$
$$\text{Luminance} = 70 \times \text{LUM}$$

where 1955, 5533, and 70 are the scale factors for the three axes; 0.6568 and 0.01825 are the *r* and *b* coordinates of illuminant C; and LUM corresponds to the

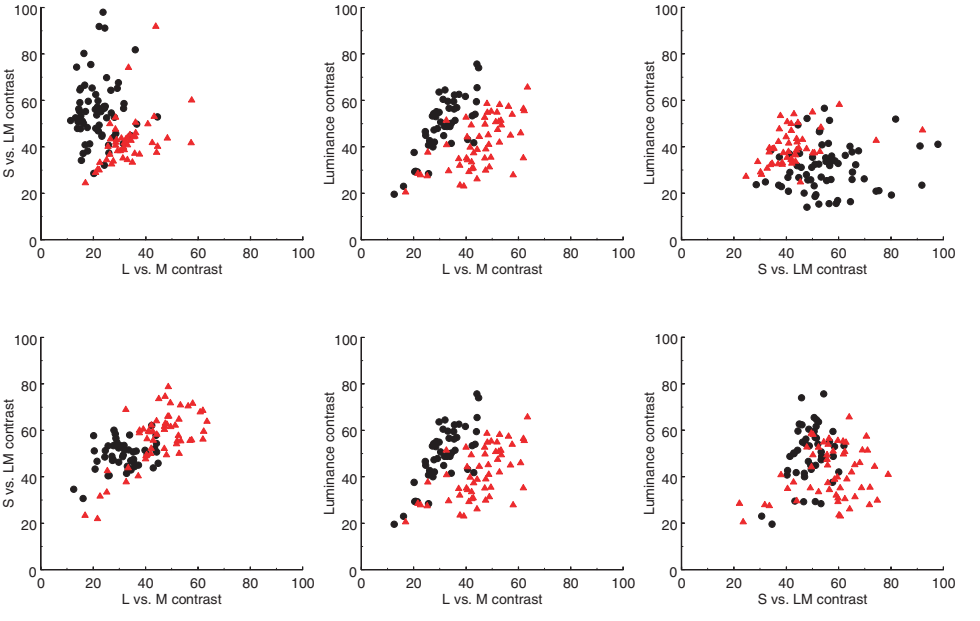

Figure 6. Chromatic and luminance contrasts in individual scenes measured during wet (black symbols) or arid (red symbols) seasons. Plots compare the distribution of rms contrasts within earth regions along the *L* vs. *M* or *S* vs. *LM* chromatic axes (left), or each chromatic axis relative to the luminance contrast in the images (middle and right). The upper panels were for scenes in India while the lower panels were for the scenes in Dog Valley.

luminance contrast relative to the mean luminance in the image $[(I - I_{mean})/I_{mean}]$. This scaling is based on empirical measurements of sensitivity to contrasts along the three axes and thus has the advantage of more nearly equating the perceptual salience of signals along the axes (Webster and Mollon 1994). The rms contrasts for individual scenes based on this scaling are compared for different pairs of cardinal axes in Figure 6 for the scenes from India and Dog Valley. This shows that the scaling factors we used give roughly comparable weight to contrasts along the three dimensions, though they somewhat overestimate the ''effective'' variance along the *S* vs. *LM* axis for the scenes in India. A similar result was found by Webster and Mollon (1997). Finally, the distribution of contrasts within the scaled space was analyzed to determine the color-luminance direction that accounted for the most variance in the contrasts.

Figure 7 plots the principal axes for each location at each measurement time. In these plots the *x* axis gives the chromatic angle within the plane defined by the scaled *L* vs. *M* axis (0–180°) and the *S* vs. *LM* axis (90–270°). The *y* axis gives the color-luminance angle or elevation out of the chromatic plane (0°) and toward the achromatic axis (−90 to +90°). Large symbols plot the first principal axis for each scene while the small symbols plot the second orthogonal axis. The third axis (not shown) is constrained to be orthogonal to the first two and typically had an elevation near 0°, suggesting that the distributions are, to a first approximation, characterized by planes perpendicular to the isoluminant plane (Webster and Mollon 1997). The chromatic axes of the distributions span a limited range, from

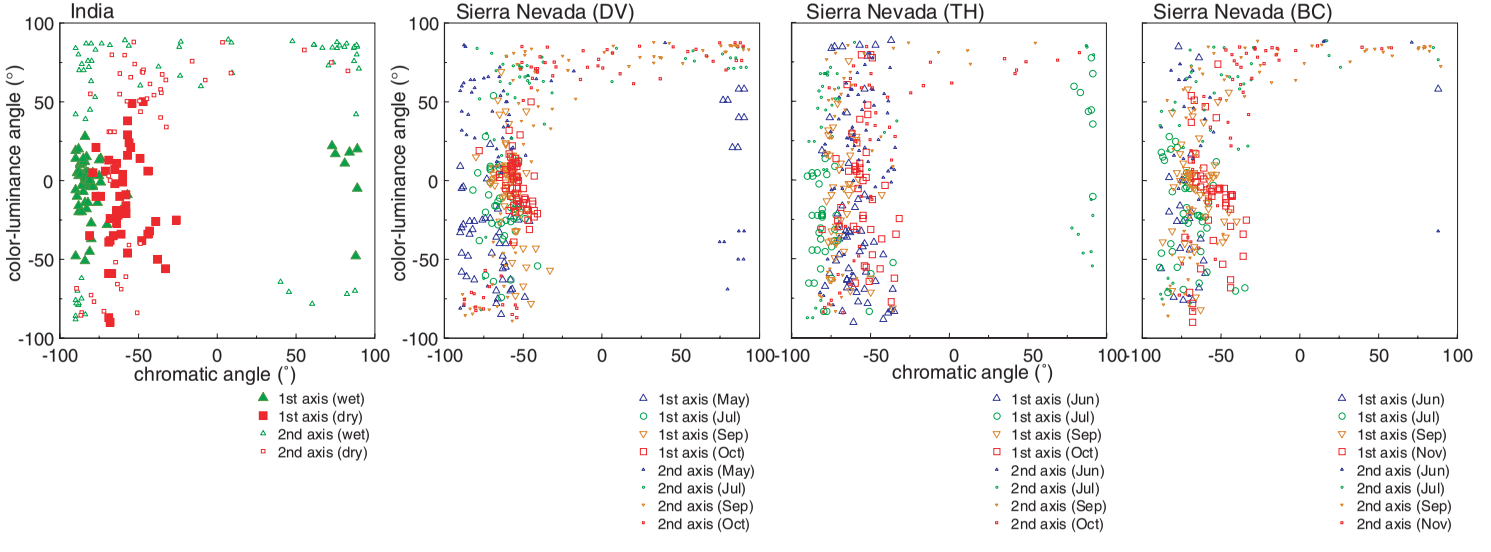

Figure 7. Principal axes for the color distributions from earth regions within individual scenes. Large symbols show the dominant axis of the variation in each scene as measured along the x axis by the chromatic angle within the L vs. M (0°) and S vs. LM (−90 and +90) plane, and by the tilt out of the chromatic plane (0°) toward the luminance axis (−90 and +90). Symbol colors show the axes measured at the different time periods. Small symbols plot the second, orthogonal axis of the distributions. The left panel is for scenes in India while the remaining panels are for the three locations in the Sierras.

roughly −90° (the *S* vs. *LM* axis) to angles of roughly −45°, a blue–yellow axis intermediate to the *S* vs. *LM* and *L* vs. *M* cone-opponent axes. While the nominal angles of the axes depend on the metric for defining the color space, it is notable that (within any space) the range of the angles is bounded by two theoretically important and readily distinguishable axes: the cardinal *S* axis of early color coding and the unique blue–yellow axis of color appearance.

This pattern is very similar to the results reported by Webster and Mollon (1997) for the set of scenes they sampled. However, the present results more clearly reveal the basis for these color changes. First, it is evident from the figures that at each location the dominant chromatic axis shifts systematically with the season. During wet periods of more lush vegetation the color variation is primarily along the *S* vs. *LM* axis, but shifts progressively toward the blue–yellow axis over time. Second, the present analysis shows that the changes in the color distributions are a characteristic of the terrestrial environment itself and not how the mean color of the earth changes relative to sky. That is, a shift from green to yellow in the foliage might itself introduce a correlation between the cone-opponent axes owing to an average change in the scene colors compared to the more static colors of the sky. However, the change in the principal axes is similarly pronounced when the sky is excluded. This is likely to occur because the foliage color is shifting relative to more static and neutral reflectances such as for soils and bark (Hendley and Hecht 1949; Osorio and Bossomaier 1992).

Figure 8 illustrates the variations within the distributions a second way, by showing the correlations between the signals along the *L* vs. *M*, *S* vs. *LM*, and luminance axes. These are again restricted to measurements based on the terrestrial regions in the images. The correlations vary widely among individual scenes, but nevertheless again show a characteristic pattern for each location. During drier periods there is a strong negative correlation between the *L* vs. *M* and *S* vs. *LM* chromatic signals, averaging −0.44 in India during the winter season and −0.60 in the Sierras in the final fall measurements. This is consistent with the pronounced blue–yellow bias in the scenes. The correlations are reduced during the wet seasons, but are still present (averaging −0.27 for India and −0.28 for the Sierras). Thus, for either location there is no period at which the cardinal chromatic axes capture fully independent information about color in the scenes. In contrast, the correlations between either chromatic axis and luminance is on average much weaker (but still substantial within some individual scenes) and shows less shift with the climate change.

The preceding analyses show that there are large and consistent shifts in the color statistics within scenes. It is interesting to ask to what extent this allows color cues to be diagnostic of the environment. To examine this, we compared the probability distributions across the seasons. These are shown in Figure 9, which plots the probability that a particular chromaticity came from a particular time period either for scenes in India (shown for monsoon vs. winter) or scenes in Dog Valley (for early spring vs. late fall). The distributions include both earth and sky. For both locations there are, again, clear swings in the colors, primarily along the *L* vs. *M* axis at low *S* values. Not surprisingly, this is again the change from green to yellow in the vegetation, but the point is that this provides a reliable cue to the season in both environments. Figure 10 pools these distributions to now compare the changes in season across both locations (lower panels) or a change in location across

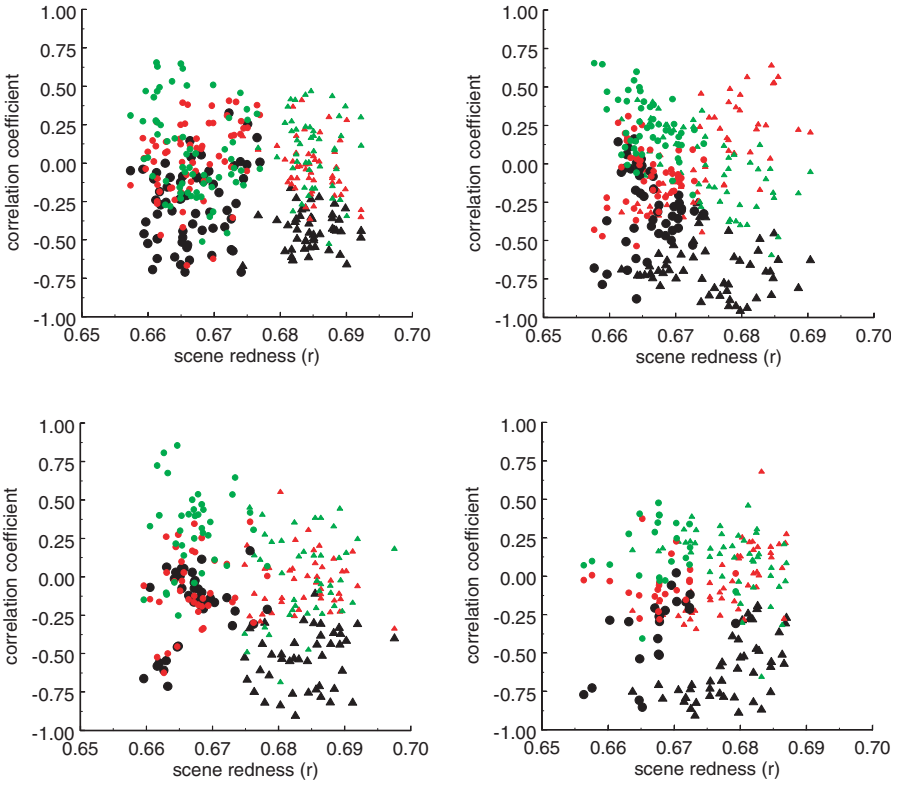

Figure 8. Correlations between the color signals along different pairs of cardinal axes: *L* vs. *M* and *S* vs. *LM* (black symbols); *L* vs. *M* and luminance (red); and *S* vs. *LM* and luminance (green). Each point plots the coefficient for a single scene as a function of the mean *L vs. M* value (*r*-value in the MacLeod–Boynton space) in the scene. Circles and triangles denote images acquired in wet or dry seasons, respectively. The left panel is for scenes in India while the remaining panels are for the three locations in the Sierras.

both seasons (upper panels). This comparison shows that the color shifts are more substantial over time than over space (for the specific locations we measured). Thus, the changes in color within the same environment over time are the principal source of variation in the color statistics of the scenes.

Discussion

The distribution of colors within natural scenes spans only a limited range of the full gamut of possible colors, yet within this range seasonal changes are nevertheless perceptually salient. Hering (in press) has recently characterized these appearance changes by visually matching the colors in outdoor landscapes in Germany. In the present study we documented these by colorimetrically sampling the distribution of colors within the same environments at different times. Our principal finding – that there are changes over time in both the mean color of scenes and how

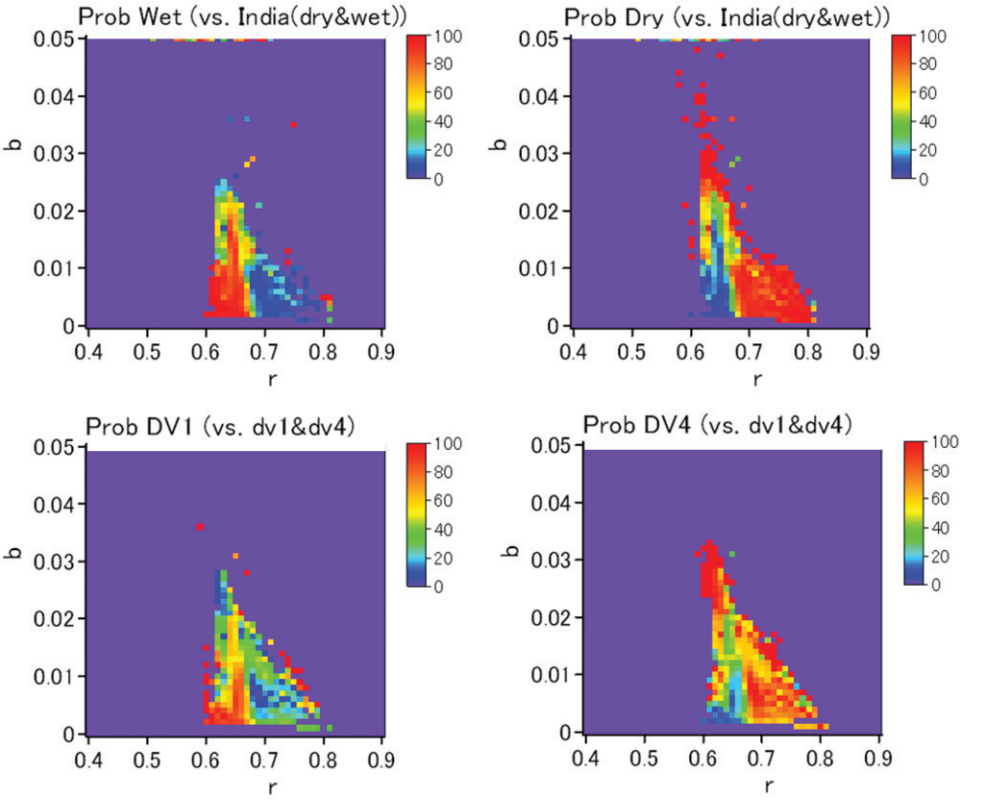

Figure 9. Comparisons of the aggregate color distributions for images measured in different seasons. Pairs of panels show the probability that a given chromaticity came from a scene in the wet (left) or dry (right) season. The top panels are for the images in India during while the bottom panels are for the images in Dog Valley.

colors within scenes vary around the mean – is at first glance trivially obvious. It is not surprising that the world is greener in the spring or wet seasons and becomes yellow in the fall or dry seasons. However, we illustrate below that the specific pattern of these color changes have a number of important implications for how color coding might be matched to color in the environment.

Before considering these, it is worth noting some of the limitations of the current study. First, we sampled only two environments and these may not be sufficiently representative of the color statistics of other ecosystems nor of the specific color context in which primate color vision evolved or color-naming patterns in humans emerged. In particular, we examined environments with large climatic changes for which temporal variations in color are pronounced. Second, within these environments our sampling of seasonal changes and in particular the time course of these changes is incomplete. Finally, the images we acquired at a particular time did not completely sample the color characteristics of the settings. For example, most images were taken with the camera directed away from the sun. When facing the sun the colors are often conspicuously different in part because of the translucence of backlit foliage.

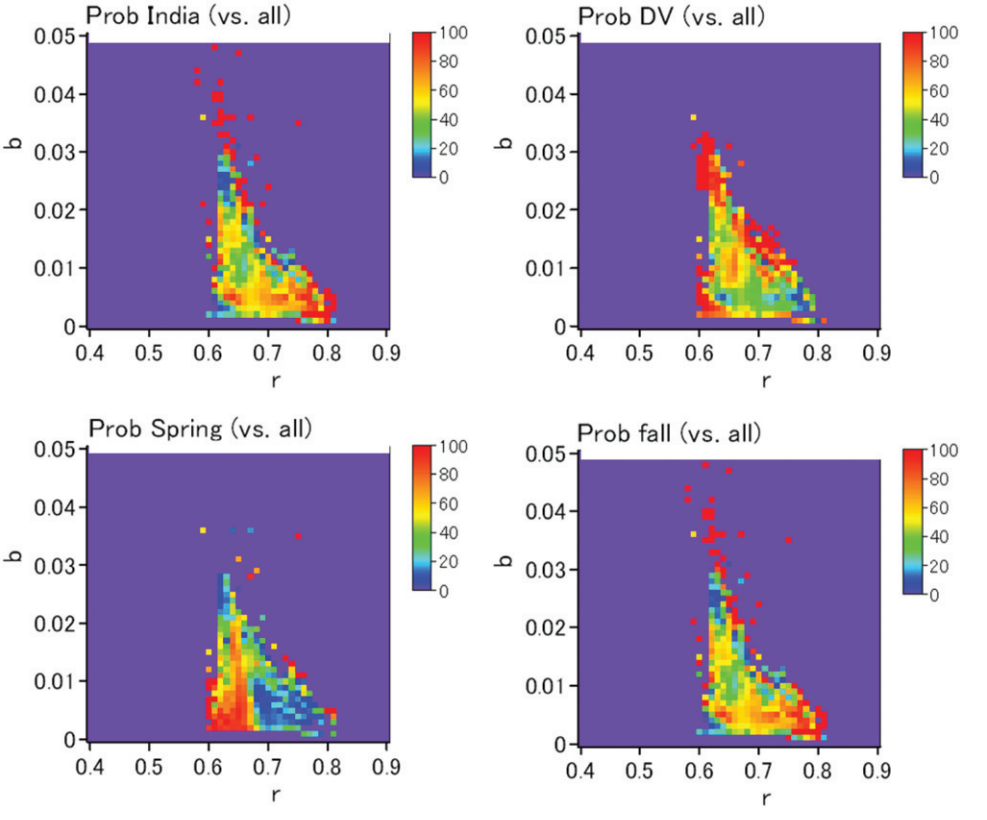

Figure 10. Comparisons of the aggregate color distributions for images measured in different seasons or at different locations. In the upper plots, the probability that a chromaticity came from India (top left) or Dog Valley (top right) is compared after pooling over both seasons. In the lower plots, the probability that a chromaticity came from a wet (left) or dry (right) season is compared after pooling over both locations.

Despite these limits, the similar patterns of color we observed for markedly different environments suggest some general conclusions. A number of studies have addressed whether visual coding is optimized to efficiently represent the variations in color in the natural environment (Webster and Mollon 1997; Ruderman et al. 1998; Párraga et al. 2002; MacLeod and von der Twer 2003; Lovell et al. 2005). As noted, early post-receptoral mechanisms are tuned to the chromatic signals given by the *L* vs. *M* and *S* vs. *LM* opponent axes. These mechanisms would thus optimally code color distributions that vary independently along these two axes. This ideal is approached for scenes dominated by lush vegetation and that include little sky (Webster and Mollon 1997; Ruderman et al. 1998; Johnson et al. 2005), which tend to show principal axes aligned roughly along the *S* vs. *LM* axis. However, for the majority of the scenes we sampled there were significantly negative correlations between the two chromatic axes (Figure 6). These persisted when regions of sky were excluded, and though weaker, also persisted in wet seasons. This negative correlation amounts to a ''blue–yellow'' bias in natural scenes and has been observed in most previous studies that have sampled very different outdoor

environments (Burton and Moorhead 1987; Webster and Mollon 1997; Ruderman et al. 1998; MacLeod and von der Twer 2003), suggesting that it is a prominent and general chromatic feature of natural images. This raises the question of to what extent, or for which specific context, color coding along the geniculate axes was driven by the general constraint of coding efficiency.

One problem in interpreting the color variations in images is that there is no obvious metric for equating the signals along different dimensions of color space (Brainard 1996). Cone contrasts are necessarily larger for luminance variations than for color and larger for the *S* vs. *LM* chromatic axis than the *L* vs. *M* axis because of the overlap of the cone sensitivities. Thus a metric like cone contrast predicts that the world varies primarily in luminance and that chromatic contrasts fall primarily along the *S* axis. However, another prediction of coding efficiency is that the dynamic range of mechanisms should be matched to the range of stimulus levels (Laughlin 1987; MacLeod and von der Twer 2003; Long et al. 2006). This suggests that contrasts should instead be scaled to equate visual sensitivity or perceptual salience for the different dimensions. This is a common approach in psychophysical studies that attempt to compare performance along different color directions (Switkes and Crognale 1999), and is the approach we used to measure the principal axes (Figures 6 and 7). Perceptually scaling the axes is itself problematic because it depends on the specific task and stimulus used to measure sensitivity (and in our case was based on equating the magnitude of contrast adaptation for different axes for low spatial and temporal frequencies; Webster and Mollon 1994). However, it is notable that the range of contrasts in the scenes we sampled are roughly comparable by this measure, and thus in this sense visual responses are roughly matched to the range of variation in scenes.

Unlike the chromatic contrasts, the correlations between luminance and color were on average much weaker, though they again varied widely and were therefore strong for some individual scenes. Thus in this case mechanisms that respond to luminance or chromatic contrast may come closer to providing an efficient representation of the ensemble color statistics of natural images. Golz and MacLeod (2002) showed that correlations between luminance and color should often occur for natural images and that these afford a potential cue for disambiguating the average color of the scene reflectances from the average color of the illuminant. Specifically, they demonstrated that scenes with surfaces that have a red bias would tend to have a more negative correlation between redness and luminance under a given illuminant. Surprisingly, these correlations were not evident in the population statistics for our images. Changes in the seasons produced a large change in the mean redness of the scenes, yet this did not clearly alter the overall relationship between *L* vs. *M* contrast and luminance contrast in the images (Figure 8).

An alternative to modeling the global efficiency of visual coding has been to relate visual mechanisms to the performance on specific visual tasks. For example, trichromacy is unique among mammals to primates, who share with other mammals an ''ancient'' dichromatic subsystem based on comparing *S* cones vs. longer wave cones, but in addition evolved a ''modern'' subsystem based on comparisons between separate *L* and *M* cones (Mollon 1989). A number of studies have explored the natural color signals that might be detected by the *L* vs. *M* chromatic contrasts. In particular, this dimension is nearly optimal for discriminating ripening fruit (Osorio and Vorobyev 1996; Regan et al. 2001; see also Sumner and Mollon 2000)

or edible leaves (Dominy and Lucas 2001; Troscianko et al. 2003) against the background of foliage, and is also the chromatic dimension that captures variations in complexion and thus the health and emotional states of conspecifics (Mollon 1989; Changizi et al. 2006; Fernandez and Morris 2007). These observations place special emphasis on detecting reddish targets or signals along the $+L$ pole of the opponent axis. In the present study, we found that this dimension also characterizes the primary change in the average chromaticity of scenes as the climate changes and leaves build up or lose their chlorophyll. Thus another potential advantage of the L vs. M signals is that they provide a measure of the general lushness of the environment, and this ''target'' is carried by the $-L$ or greenish pole of the axis. Interestingly, in a recent study in Kibale Forest, Uganda, Troscianko et al. (2003) noted that green leaves form a substantial part of the diet of foraging primates during the dry season (Troscianko et al. 2003).

Whatever their merit, speculations about the match between color coding and the color environment must be tempered by the fact that the environment itself is often cycling through changes in color. What are the implications of these stimulus variations for variations in color perception? A first point to note is that while the color changes we observed are large, they nevertheless span a limited range within the volume of color space. As Webster and Mollon (1997) reported, the color distributions appear bounded by the S vs. LM axis for lush environments or seasons and by the perceptual blue–yellow axis for arid contexts. This represents a range of $\sim 45^\circ$ out of a possible span of 180° within our scaled space. Moreover, we found that this pattern is very similar within the two environments we sampled, or in other words, that much of the color variation is intrinsic to how a given environment changes over time (Figure 10). This suggests that the color variations themselves have a restricted and characteristic pattern that may be typical of much of the natural world. Though the magnitude of this variation will obviously vary with the ecosystem, it is possible that these characteristic stimulus patterns contribute to characteristics properties of human color perception. For example, a striking feature of color naming is that the color spectrum is parsed in similar ways by the world's languages (Berlin and Kay 1969; Kay and Regier 2003). Thus most languages have a basic color term that glosses to the English ''red'' in that it denotes a very similar focal stimulus. The bases for the privileged status of basic color terms and unique hues have typically focused on the common physiology of color processing in the human visual system (Kaiser and Boynton 1996). However, as we noted in the introduction, it has not yet proven possible to identify neural mechanisms that would predict why some chromatic stimuli are more basic or perceptually special, suggesting that color categories may instead be tied to properties of the color environment. Specifically, to the extent that prominent features of the color statistics of the natural world are characteristic and vary in characteristic ways within different environments, universals in color naming may reflect universals in the color environment.

As we also noted in the introduction, one candidate environmental universal is the daylight locus, which is in close correspondence to the perceptual unique blue–yellow axis (Lee 1990; Shepard 1992; Mollon 2006). It is interesting that the color distributions in arid scenes also fall close to this axis and that it roughly defines the limit of the color changes in foliage. Thus, objects as well as illuminants in the environment might have played a role in shaping the blue–yellow dimension of color

appearance. However, this leaves as a puzzle the reason why colors along the *S* vs. *LM* axis, which vary from purple to yellow–green and also define a boundary for natural color distributions, do not appear similarly special.

If regularities in the color environment underlie consistencies in color perception, then variations in the color statistics should instead lead to differences in appearance. There are in fact large individual differences in the stimuli observers select for unique hues (Webster et al. 2000; Kuehni 2004), and again these cannot be tied to individual differences in spectral sensitivity. There are also significant differences in focal color settings between populations in different environments. For example, we have shown that observers in India, tested within regions including the locations where images for the current study were collected, differ quantitatively in their unique hue and focal color settings from a population of students in the Reno area (Webster et al. 2002b). Moreover, Webster and Kay (in press) have recently analyzed the focal color settings for the 110 languages of the World Color Survey and showed that the mean foci varied more across linguistic groups than would be predicted by the within-language variability in color naming. Thus, while languages may share a set of common color terms the exact focal stimuli for these terms can vary. One way this could arise is if individuals are adapted to the specific color distributions defining their environment. Adaptation adjusts to both the average color through chromatic adaptation and to the variance in color through contrast adaptation. This could in principle lead to selective biases in color appearance for observers exposed to environments that have a bias in their color distributions (e.g. with greater variance along the *S* vs. *LM* or blue–yellow axis) (Webster and Mollon 1997). However, it remains unknown to what extent the differences in color naming across different populations reflect environmental vs. cultural differences.

The large, slow drifts in color with the seasons have important implications for visual adaptation and how this might calibrate color appearance. Most studies of adaptation have focused on very short-term exposures to changes in the stimulus, but adaptation may also act on long-time scales to adjust to changes in the observer or the environment. For example, the density of lens pigment increases with age leading to progressive losses in sensitivity to short wavelength light. Adaptation may be important to discount this sensitivity change so that color appearance remains stable (Werner and Schefrin 1993). Delahunt et al. (2004) examined these processes by measuring changes in achromatic settings after cataract surgery. Removing the cataractous lens effectively floods the retina with shortwave light. Immediately after surgery this causes the world to appear blue, yet the white settings slowly renormalize over a period of many weeks to return toward the patient's original neutral point. Long-term drifts in unique yellow have also been found following long-term exposure to biased color environments (Neitz et al. 2002). Note that these long-term changes reflect a shift in the underlying, ''intrinsic'' sensitivity of the visual system and are distinct from the rapid adjustments that occur in response to the currently viewed stimulus. The specific time course of these long-term adjustments is not well-characterized, nor is it known whether similar long-term effects occur for other properties of the distributions such as contrast. If they are rapid enough to track the mean changes in chromaticity across the seasons then achromatic settings should cycle with the seasons. Alternatively, it may be that the intrinsic changes in sensitivity that are reflected in studies of long-term adaptation

are intentionally sluggish enough to integrate over the cyclical changes in the environment. We are currently exploring these alternatives.

The recalibration of achromatic settings with aging suggests that white is set by a consistent feature of the environment, yet it is not clear what this feature is or how visual coding adjusts in response to it. One candidate is adaptation to the average spectral stimulus the observer is exposed to. By this account, terrestrial regions in most images are too yellow or green to determine the achromatic point, which instead falls at a chromaticity intermediate to earth and sky. This suggests that the sky, which is often considered an inconsequential property of color in images, actually plays a significant role in calibrating color vision (MacLeod and von der Twer 2003). The processes underlying the white point must act locally, since they compensate for the spatial inhomogeneities of the retina, for example, correcting the differences in spectral sensitivity owing macular pigment (Beer et al. 2005; Stringham and Hammond 2007). This could arise if each retinal region is locally adapted to the same external stimulus. Recently we found that the chromaticity that appears white to an observer is the same stimulus that maintains an unbiased state in chromatic adaptation (Webster et al. 2007). This implies that the perceptual norm or neutral point for color does in fact reflect a response norm or neutral point in chromatic mechanisms (at the sites at which chromatic adaptation affects the visual response). A local sensitivity regulation of this kind can discount differences in spectral sensitivity by normalizing color coding for the same environmental stimulus, but should lead to differences in color appearance if different parts of the retina are exposed to different average colors. In particular, the upper and lower retina are more often exposed to earth or sky, and white settings might therefore be expected to vary in predictable ways across the visual field. Measurements of such effects might help to establish how color perception is controlled by the statistics of the color environment.

Acknowledgment

This work was supported by EY-10834.

References

Attewell D, Baddeley R. 2007. The distribution of reflectances within the visual environment. Vision Res 47:548–554.

Beer RD, Wortman J, Horwitz G, MacLeod DIA. 2005. Compensation of white for macular filtering. J Vision 5:282a.

Berlin B, Kay P. 1969. Basic color terms: Their universality and evolution Berkeley: University of California Press.

Brainard DH. 1996. Cone contrast and opponent modulation color spaces. In: Kaiser P, Boynton RM, editors. Human color vision. Washington DC: Optical Society of America. pp 563–579.

Brainard DH, Roorda A, Yamauchi Y, Calderone JB, Metha A, Neitz M, Neitz J, Williams DR, Jacobs GH. 2000. Functional consequences of the relative numbers of L and M cones. J Opt Soc Am A 17:607–614.

Brelstaff G, Párraga A, Troscianko T, Carr D. 1995. Hyperspectral camera system: Acquisition and analysis. SPIE 2587:150–157.

Brown RO. 1994. The world is not grey. Invest Ophthalmol Visual Sci (Suppl.) 35:2165.

Burton GJ, Moorhead IR. 1987. Color and spatial structure in natural scenes. Appl Opt 26:157–170.
Changizi M, Zhang Q, Shimojo S. 2006. Bare skin, blood and the evolution of primate colour vision. Biol Lett 22:217–221.
Delahunt PB, Webster MA, Ma L, Werner JS. 2004. Long-term renormalization of chromatic mechanisms following cataract surgery. Visual Neurosci 21:301–307.
Derrington AM, Krauskopf J, Lennie P. 1984. Chromatic mechanisms in lateral geniculate nucleus of macaque. J Physiol 357:241–265.
Doi I, Inui T, Lee T-W, Wachtler T, Sejnowski TJ. 2003. Spatio-chromatic receptive field properties derived from information-theoretic analyses of cone mosaic responses to natural scenes. Neural Comput 15:397–417.
Dominy NJ, Lucas PW. 2001. Ecological importance of trichromatic vision to primates. Nature 410:363–366.
Fernandez AA, Morris MR. 2007. Sexual selection and trichromatic color vision in primates: Statistical support for the pre-existing-bias hypothesis. Am Nat 170:10–20.
Golz J, MacLeod DIA. 2002. Influence of scene statistics on colour constancy. Nature 415:637–640.
Hendley CD, Hecht S. 1949. The colors of natural objects and terrains, and their relation to visual color deficiency. J Opt Soc Am 39:870–873.
Hering B. In press. Seasonal changes in dominating hues in landscapes close to nature. Proceedings of the international conference on color harmony. Budapest: Hungarian Academy of Sciences.
Johnson AP, Kingdom FA, Baker CL. 2005. Spatiochromatic statistics of natural scenes: First- and second-order information and their correlational structure. J Opt Soc Am A 22:2050–2059.
Kaiser P, Boynton RM. 1996. Human color vision USA: Optical Society of America.
Kay P, Regier T. 2003. Resolving the question of color naming universals. Proc Natl Acad Sci 100:9085–9089.
Krauskopf J, Williams DR, Heeley DW. 1982. Cardinal directions of color space. Vision Res 22:1123–1131.
Kuehni RG. 2004. Variability in unique hue selection: A surprising phenomenon. Color Res Appl 29:158–162.
Laughlin SB. 1987. Form and function in retinal processing. Trends Neurosci 10:478–483.
Lee H-C. 1990. A computational model for opponent color encoding. Advanced printing of conference summaries, SPSE's 43rd annual conference. New York: Rochester.
Long F, Yang Z, Purves D. 2006. Spectral statistics in natural scenes predict hue, saturation, and brightness. Proc Natl Acad Sci 103:6013–6018.
Lovell P, Tolhurst D, Parraga C, Baddeley R, Leonards U, Troscianko J, Troscianko T. 2005. Stability of the color-opponent signals under changes of illuminant in natural scenes. J Opt Soc Am A 22:2060–2071.
MacLeod DIA, Boynton RM. 1979. Chromaticity diagram showing cone excitation by stimuli of equal luminance. J Opt Soc Am 69:1183–1186.
MacLeod DIA, von der Twer T. 2003. The pleistochrome: Optimal opponent codes for natural colours. In: Mausfeld R, Heyer D, editors. Colour perception: Mind and the physical world. Oxford: Oxford University Press. pp 155–184.
Maloney LT. 1986. Evaluation of linear models of surface spectral reflectance with small numbers of parameters. J Opt Soc Am A 3:1673–1683.
Miyahara E, Pokorny J, Smith VC, Baron R, Baron E. 1998. Color vision in two observers with highly biased LWS/MWS cone ratios. Vision Res 38:601–612.
Mizokami Y, Werner JS, Crognale MA, Webster MA. 2006. Nonlinearities in color coding: Compensating color appearance for the eye's spectral sensitivity. J Vision 31:996–1007.
Mollon JD. 2006. Monge: The Verriest lecture, Lyon, July 2005. Visual Neurosci 23:297–309.
Mollon JD. 1989. Tho' she kneel'd in that place where they grew. J Exp Biol 146:21–38.
Nagle MG, Osorio D. 1993. The tuning of human photopigments may minimize red-green chromatic signals in natural conditions. Proc Roy Soc Lond B 252:209–213.
Nascimento S, Ferreira F, Foster DH. 2002. Statistics of spatial cone-excitation ratios in natural scenes. J Opt Soc Am A 19:1484–1490.
Neitz J, Carroll J, Yamauchi Y, Neitz M, Williams DR. 2002. Color perception is mediated by a plastic neural mechanism that is adjustable in adults. Neuron 35:783–792.
Osorio D, Bossomaier TRJ. 1992. Human cone-pigment spectral sensitivities and the reflectances of natural surfaces. Biol Cybernetics 67:217–222.

Osorio D, Vorobyev M. 1996. Colour vision as an adaptation to frugivory in primates. Proc Roy Soc Lond B 263:593–599.
Paramei GV, Dedrick D, editors. The anthropology of colour: Interdisciplinary multilevel modelling. John Benjamins: Amsterdam.
Párraga CA, Troscianko T, Tolhurst DJ. 2002. Spatiochromatic properties of natural images and human vision. Curr Biol 12:483–487.
Philipona DL, O'Regan JK. 2006. Color naming, unique hues, and hue cancellation predicted from singularities in reflection properties. Visual Neurosci 23:331–339.
Polyak S. 1957. The vertebrate visual system Chicago: University of Chicago Press.
Regan BC, Julliot C, Simmen B, Vienot F, Charles-Dominique P, Mollon JD. 2001. Fruits, foliage and the evolution of primate colour vision. Phil Trans Roy Soc Lond, Series B 356:229–283.
Regier T, Kay P, Khetarpal N. 2007. Color naming reflects optimal partitions of color space. Proc Natl Acad Sci 104:1436–1441.
Ruderman DL, Cronin TW, Chiao C-C. 1998. Statistics of cone responses to natural images: Implications for visual coding. J Opt Soc Am A 15:2036–2045.
Schefrin BE, Werner JS. 1990. Loci of spectral unique hues throughout the life span. J Opt Am A 7:305–311.
Shepard RN. 1992. The perceptual organization of colors: An adaptation to regularities of the terrestrial world? In: Barkow J, Cosmides L, Tooby J, editors. The adapted mind. Oxford: Oxford University Press. pp 495–532.
Smith VC, Pokorny J. 1975. Spectral sensitivity of the foveal cone photopigments between 400 and 500 nm. Vision Res 15:161–171.
Stringham JM, Hammond BR Jr. 2007. Compensation for light loss due to filtering by macular pigment: Relation to hue cancellation. Ophthalmic Physiol Optics 27:232–237.
Sumner P, Mollon JD. 2000. Chromaticity as a signal of ripeness in fruits taken by primates. J Exp Biol 203:1987–2000.
Switkes E, Crognale MA. 1999. Comparison of color and luminance contrast: Apples versus oranges? Vision Res 39:1823–1831.
Troscianko T, Baddeley R, Parraga CA, Leonards U, Troscianko J. 2003. Visual encoding of green leaves in primate vision (Abstract). J Vision 3:137a.
Webster MA, Malkoc G, Bilson AC, Webster MA. 2002a. Color contrast and contextual influences on color appearance. J Vision 2:505–519.
Webster MA, Miyahara E, Malkoc G, Raker VE. 2000. Variations in normal color vision. II: Unique hues. J Opt Soc Am A 17:1545–1555.
Webster MA, Mollon JD. 1994. The influence of contrast adaptation on color appearance. Vision Res 34:1993–2020.
Webster MA, Mollon JD. 1997. Adaptation and the color statistics of natural images. Vision Res 37:3283–3298.
Webster MA, Webster SM, Bharadwadj S, Verma R, Jaikumar J, Madan G, Vaithilingam E. 2002b. Variations in normal color vision III: Unique hues in Indian and United States observers. J Opt Soc Am A 19:1951–1962.
Webster MA, Yasuda M, Haber S, Leonard D, Ballardini N. 2007. Adaptation and perceptual norms. In: Rogowitz BE, Pappas TN, Daly SJ, editors. Human vision and electronic imaging XII. SPIE 6492-1S: pp 1–11.
Werner JS, Schefrin BE. 1993. Loci of achromatic points throughout the life span. J Opt Soc Am A 10:1509–1516.
Yendrikhovskij SN. 2001. Computing color categories from statistics of natural images. J Imaging Sci Technol 45:409–417.